Procedia Computer Science

Volume 51, 2015, Pages 2493–2502

ICCS 2015 International Conference On Computational Science

Spectral Validation of Measurements in a Vehicle Tracking DDDAS

Burak Uzkent[1], Matthew J. Hoffman[2], and Anthony Vodacek[1]

[1] Chester F. Carlson Center for Imaging Science, Rochester Institute of Technology, Rochester, New York, USA
bxu2522@rit.edu, vodacek@cis.rit.edu

[2] School of Mathematical Sciences, Rochester Institute of Technology, Rochester, New York, USA
mjhsma@rit.edu

Abstract

Vehicle tracking in adverse environments is a challenging problem because of the high number of factors constraining their motion and possibility of frequent occlusion. In such conditions, identification rates drop dramatically. Hyperspectral imaging is known to improve the robustness of target identification by recording extended data in many wavelengths. However, it is impossible to transmit such a high rate data in real time with a conventional full hyperspectral sensor. Thus, we present a persistent ground-based target tracking system, taking advantage of a state-of-the-art, adaptive, multi-modal sensor controlled by Dynamic Data Driven Applications Systems (DDDAS) methodology. This overcomes the data challenge of hyperspectral tracking by only using spectral data as required. Spectral features are inserted in a feature matching algorithm to identify spectrally likely matches and simplify multi-dimensional assignment algorithm. The sensor is tasked for spectra acquisition by the prior estimates from the Gaussian Sum Filter and foreground mask generated by the background subtraction. Prior information matching the target features is used to tackle false negatives in the background subtraction output. The proposed feature-aided tracking system is evaluated in a challenging scene with a realistic vehicular simulation.

Keywords: vehicle tracking, efficient outlier exclusion, spectral features, multi-modal sensor

1 Introduction

Aerial surveillance in urban environments has been extensively studied in the literature. Most of them try to tackle tough tracking problems with limited information. A large volume of studies focus on using Ground Moving Target Indicator radars, which measure the locations of moving ground objects as well as their doppler velocities, to tackle problems in ground target tracking [1, 11, 6, 7, 15]. With radar, however, we are limited to kinematic information to achieve persistent tracking, and kinematic data alone is very likely to fail in challenging situations due to occlusions, parallax, or clutter. To achieve a more robust system, one can consider utilizing unique fingerprints of objects in addition to the kinematic data. The Dynamic Data-Driven Applications Systems (DDDAS) framework is perfectly

Selection and peer-review under responsibility of the Scientific Programme Committee of ICCS 2015

doi:10.1016/j.procs.2015.05.358

suited for allowing the tracking application to manage the control of the runtime reconfiguration of the sensor to collect the most beneficial data and the feedback of this data into an adaptive modeling framework for the dynamic scene.

Most of the narrow-area surveillance studies extract local features from the scene to identify their targets. These features can be texture, color histogram, SIFT, optical flow, edges, or corners [18, 14, 19]. However, in a wide-area ground-based tracking system, one can not rely on these features due to low resolution. Instead, the hyperspectral data sampled from a single pixel of a target of interest (TOI) can be beneficial since it provides a unique fingerprint. Hyperspectral imaging involves of acquiring data in hundreds of narrow adjacent spectral bands. Thus, by inserting extended data, classification of objects can be further improved. It is impossible to transmit the volume of data from a conventional full hyperspectral sensor in real time tracking. However, with the recent advancements in the sensor technology, it becomes possible to quickly collect only desired spectral data [10]. As a result, such a sensor in fact can be employed in a real time tracking system. Employing an adaptive sensor requires DDDAS-based tools for determining the locations and modalities most useful for the the tracker at a given time and controlling the realtime reconfiguration of the sensor to collect the requested data.

In this paper, a persistent target tracking system utilizing an adaptive optical multi-modal sensor is proposed. Since some portion of spectral data to be recorded is determined by the performance of the filter, the executing tracker request external data from OpenStreetMap to acquire an intersection mask of the scene where the true target density can be multi-modal. This way we can gain prior knowledge of a possible maneuver and the tracker then adaptively can tune the transition models. However, abrupt motion changes still might result in highly nonlinear true target densities. In these cases, it is extremely challenging to collect spectra at the TOI pixels by relying on prediction-based spatial sampling. Hence, we perform measurement-based sampling in addition to the prediction-based sampling to maximize the likelihood of collecting data from the TOI.

2 Tracking System and Sensor Resource Management

A sensor capable of collecting spatial and spectral data is required to perfom high rate tracking of objects of interest. For this reason, Rochester Institute of Technology Multi-object Spectrometer (RITMOS) is considered as an adaptive performance-driven sensor together with a performance-driven algorithm to detect, identify and track targets in highly cluttered scenes [10]. RITMOS utilizes a micromirror array to reflect the light to the one of two sensors; spectrograph and panchromatic channel. The switch from panchromatic to spectral data mode for a pixel can happen very fast due to the compactness and speed of micromirror arrays. To capture the panchromatic image of the scene, an array of micromirrors reflect the light to a panchromatic imaging array. Individual micromirrors imaging the object are then tilted to reflect the light and collect the full spectrum of a specified pixel. All these configurations can be performed in real time using DDDAS algorithms.

The performance-driven tracking algorithm needs to be designed in a way that it meets the specifications of RITMOS. RITMOS requires about $0.1 - 0.125$ s to obtain panchromatic image of a scene. On the other hand, the full spectrum of a single pixel in the visible to near infrared wavelength takes 1 ms. Spatial and spectral data can not be collected simultaneosly. The frame rate 1 s is used in this study, meaning that track estimates are updated at every second. Panchromatic images are used to accomplish motion segmentation. While the sensor collects a panchromatic image, the tracking algorithm outputs the prior results that will be fed to the sensor resource management system for spectral data acquisition. Full spectral data for 100 pixels can be collected in about 0.1 s. Tracking system workflow can be seen in Fig.1.

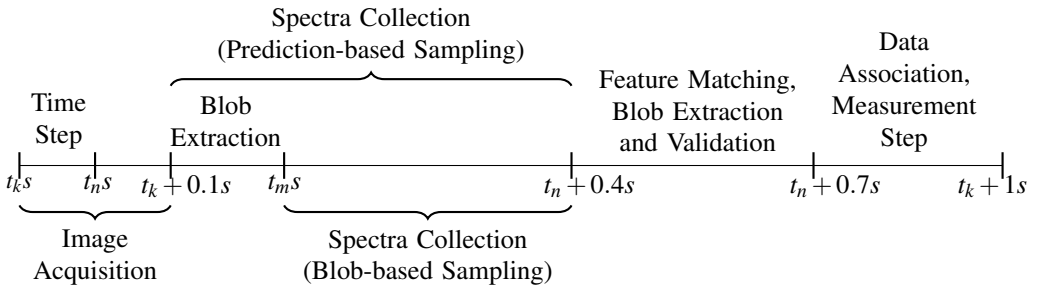

Figure 1: The workflow of the proposed tracking system using a performance-driven sensor.

3 Scenarios

To develop and test the system in a controlled environment that allows us a knowable ground truth, we use synthetic imagery generated by the Digital Imaging and Remote Sensing Image Generation (DIRSIG) model [5]. In addition, the Simulation of Urban Mobility (SUMO) traffic simulator has been integrated with DIRSIG to produce dynamic imagery for tracking scenarios [8]. The scenario used in this paper comes from DIRSIG Megascene I, which is built to resemble part of Rochester, NY, USA. The simulation uses hyperspectral imaging from a fixed aerial platform assuming a static sensor mount. The spectral range is 400 to 1000 nm with a spectral resolution of 10 nm. Thus, generated synthetic images have 61 wavelength bands. Eighty six vehicles are placed in the 130 seconds long simulation. Among them, we will focus on tracking four vehicles at separate runs.

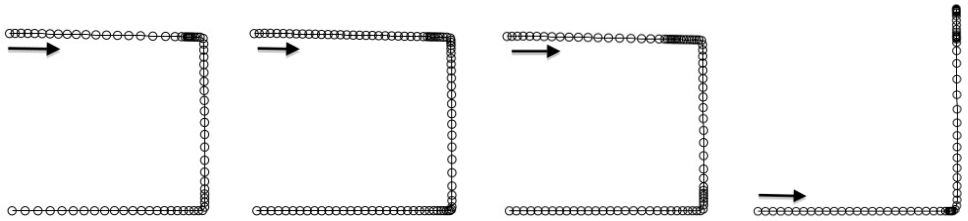

Figure 2: Trajectories of the vehicles to be tracked.

Synthetic spectral data is extremely helpful for the reasons mentioned before, however, it is crucial to simulate data matching real-world phenomenology. DIRSIG output has to be further processed to meet this need. DIRSIG yields sensor reaching radiance output relative to sensor specifications such as aperture width. The ultimate goal is to process sampled data obtained by a representative of a real world imaging scpectrometer. This process converts the sensor reaching radiance values ($\frac{Watt}{cm^2.m}$) into the digitally sampled values (*Volt*). In this process, we account for factors that exist in real-world phenomenology such as filter effects, shot noise, readout noise, integration time, detector elements, and analog to digital converters. An extensive treatment on this radiometric sampling process is given in [13].

4 Motion Segmentation

This step provides us measurements that are associated to the tracks to correct prior estimations. In this study, we use the background subtraction technique on the panchromatic images from RITMOS. Background subtraction is a simple technique that subtracts two frames to detect moving objects. These two frames are the current frame $I(x,y,k)$ at time k and the background frame $I_B(x,y)$ for x and y coordinates of each pixel. The result $I_D(x,y,k) = abs(I(x,y,k) - I_B(x,y))$ is generaly applied an empirical threshold. We apply the Median filter to the previous $n-1$ number of frames in addition to the current frame to generate a reference frame I_B as

$$I_B(x,y) = median\{I(x,y,k-i)\}, \quad i = 0,1,...,n-1. \tag{1}$$

The Median filter is a computationally efficient method which makes it eligible for our tracking system. It is especially applicable for background dominated scenes and it perfectly fits in our system since we only perform vehicular simulation. In this study, we consider 9 previous scans in addition to the current scan to generate a background mask. In fig. 3, you can see the generated background and foreground mask at a time step in the given scenario.

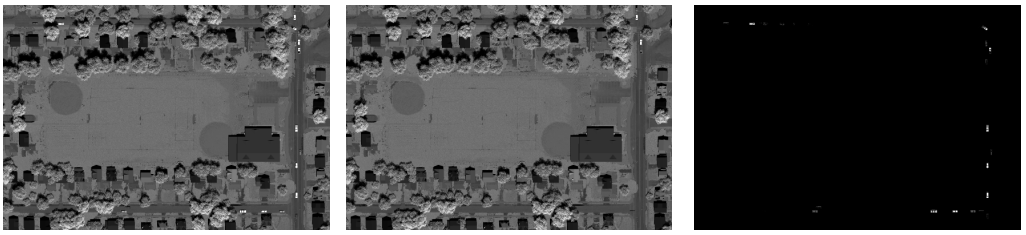

(a) (b) (c)

Figure 3: (a) Panchromatic image (I) at k , (b) background mask generated by Median filtering multiple frames ($n = 10$), I_B, (c) foreground mask after background subtraction, I_D.

The resultant difference image (fig.3c) is applied an empirically predetermined threshold. Next, we apply the morphological closing operation to remove the noise due to lighting changes, tiny nonstationary objects, and other sources and fill in the gaps.

The second step in the motion segmentation is deriving a possible true measurement for a target based on the prior estimates matching the target features. By relying on the uniqueness of spectral features we can tackle possible false negatives in the background subtraction algorithm. Overall foreground mask is estimated by adding the global foreground mask from the background subtraction and local foreground mask from the feature matching as in fig. 4. Finally, the connected component analysis is applied to uniquely label extracted blobs.

5 Gaussian Sum Kalman Filter

The GSF represents a non-Gaussian distribution by a finite mixture of Gaussian distrubutions. It allows us to implement a multiple model set strategy that can be crucial in multi-modal true target density cases. The GSF together with intersection network concept might lead to an adaptive multiple model set strategy in the junctions. This way, nonlinear true target density in the intersections can be better approximated which in turn results in directing the sensor to collect useful spectral features. The state-space and covariance matrix of each density kernel is updated by a linear or nonlinear recursive,

(a) (b) (c) (d)

Figure 4: (a) A foreground mask generated by the background subtraction method, (b) pixels from four different prior Gaussians whose spectra match the TOI, (zoomed on the targeted area) (c) the prediction-based foreground mask for the TOI after averaging the prior Gaussians in (b), (d) final foreground mask.

Bayesian estimator such as the Kalman filter (KF), Extended Kalman filter (EKF), or Unscented Kalman filter (UKF). We have both linear and nonlinear models, thus, the KF will be used to transit Gaussians with linear models whereas the EKF is used for nonlinear ones.

Assume we have a process and observations, X_{k-1} and $Y_{k-1} = \{y_{k-1}|i = 1,2,...,k-1\}$, the uncertainty $P_{k|k-1}$ associated with the state vector X_k is determined by $p(X_k|Y_{k-1})$. The GSF estimates the prior mean and uncertainty of the mixture as

$$x_{k|k-1} = \Sigma_{n=1}^{N} w_{k-1}^{n}(X_{k-1|k-1}^{n}), \tag{2}$$

$$p_{k|k-1} = \Sigma_{n=1}^{N} w_{k-1}^{n}([P_{k-1|k-1}^{n}(X_{k-1|k-1}^{n} - x_{k|k-1})(x_{k|k-1} - X_{k-1|k-1}^{n})^{T}] \tag{3}$$

where $x_{k|k-1}$ and $p_{k|k-1}$ are the expected mean and covariance of the prior mixture and w_{k-1}^{n} and N represent the weight for the nth Gaussian kernel and number of kernels. The expected mean and covariance of the posterior density $p(X_k|Y_k)$ is estimated in the same way. A more detailed documentation of the GSF in a similar adaptive multi-modal sensor-inspired tracking system is explained in [16, 17].

6 Spectral Feature-Aided Identification

Data association is required to successfully correct prior target density $p(X_k|Y_{k-1})$ with observations y_k. In this study, we propose a two step data association method. In the first step, we rely on the strength of spectral features to eliminate spectrally unlikely validated measurements within a gate drawn by the filter. By doing so, we can both decrease the complexity of the cost function and increase identification accuracy. In the next step, a multi-dimensional assignment algorithm (MDA) is employed to formulate the assignment problem [4].

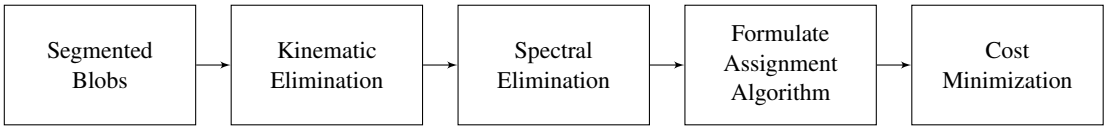

Figure 5: Target classification workflow.

6.1 Validating Measurements via Spectral Features

Two kinds of spatial sampling are performed to feed the sensor for spectral data acquisition. The first is prediction-based spatial sampling. In this case, the sensor is tasked to collect spectral data without any prior knowledge of segmented blobs. Therefore, sampling is performed by taking a subset of the pixels from where the filter predicts the target will be. This process is repeated for each Gaussian,

$X^n_{k|k-1} = \{n = 1,2,..N\}$, in the GSF. The Gaussians that spectrally match the TOI are averaged to get an additional blob on top of the segmented blobs generated by the background subtraction step as in fig. 4. The second one is measurement-based sampling. This sampling process is implemented with the knowledge of segmented blobs. The sensor is tasked to collect full spectra at the pixels in the vicinity of a blob centroid. The second step can be very beneficial in the non-Gaussian target density case since the prediction-based sampling might fail in collecting target data. The Spectral Angle Mapper (SAM) is used to measure the similarity of spectral vectors. An extensive treatment on the SAM metric can be found in [16]. The proposed algorithm to spectrally validate measurements is displayed below.

Form feature matrix D^b_k for each filter-validated foreground blob $b = 1,...,B$;
for $t = k-1,...,2$ **do**
  if *the target is not lost at t* **then**
    $F^b_k \longleftarrow mean\{min\{SAM(D^b_k, D^{match}_t)\}, min\{SAM(D^b_k, D^{user}_1)\}\}$;
    for $b = 1,...,B$ **do**
      if $F^b_k > SAM\ Threshold$ **then**
        eliminate it;
      end
    end
    break;
  end
end

Algorithm 1: The proposed feature matching algorithm for blob elimination.

6.2 Data Association

The MDA algorithm, first proposed by [12], considers S number of past scans to formulate the data association problem. This is why it is also named as the $S-D$ assignment algorithm. In 2-D case, only the current scan, k, is used for assignment. This computationaly cheap method suffers from two major drawbacks: the lack of time depth and information on target motion evolution. By considering a sufficient number of scans ($S > 2$), a data association algorithm may be able to better approximate the evolution of the target trajectory. This way, the time depth issue is resolved. Also, we can improve false assignments with upcoming measurements. This is especially beneficial in maintaining the track in challenging scenarios. By doing so, the decisions are softened. The major drawback of this approach is that it is a non-deterministic polynomial time hard (NP-hard) problem for $S \geq 3$ whereas the 2-D assignment algorithm can be solved in quasi-polynomial time. This method becomes infeasible for real time tracking with an increasing number of tracks ($v > 10$). However, it fits perfectly in our system since we are interested in single ($v < 2$), user selected target and simplify the minimization problem by reducing the number of filter-validated measurements through feature matching ($F^b_k > Threshold$).

We will provide a brief overview of how the MDA is implemented in our case. Extensive documentation on it can be found in [7]. A binary assignment variable s is defined as

$$s(k, \{y_s\}^k_{s=k-S+2}, v) = \begin{cases} 1 & y_k, y_{k-1}, ..., y_{k-S+2} \text{ is assigned to } T^v(k-S+1) \\ 0 & otherwise \end{cases}, \quad (4)$$

where $y_s = 0,1,...,M(s)$ and $v = 0,1$. M denotes the spectrally validated measurement list at scan s and $y_s = 0$ and $v = 0$ corresponds to the dummy measurement and nonexistant target. The multi-dimensional

assignment algorithm is then formulated as

$$C(k|A) = \sum_{y_{k-S+2}=0}^{M(k-S+2)} \sum_{y_{k-S+3}=0}^{M(k-S+3)} \sum_{y_{k-S+4}=0}^{M(k-S+4)} ..... \sum_{y_k=0}^{M(k)} s(k, \{y_s\}_{s=k-S+2}^{k}, 1) c(k, \{y_s\}_{s=k-S+2}^{k}), \tag{5}$$

where A contains the candidate tuples (set of measurements) and c is the cost function that evaluates the association cost. The goal is to find the tuple $a \in A$ that minimizes the overall association cost C. The association cost formula in our case is given by

$$c(k, \{y_s\}_{s=k-S+2}^{k}) = -ln(\frac{\phi(k, \{y_s\}_{s=k-S+2}^{k}, 1)}{\phi(k, \{y_s\}_{s=k-S+2}^{k}, 0)}), \tag{6}$$

where ϕ represents the association likelihoods. For $v = 1$ and $v = 0$, it is estimated as

$$\phi(k, y_s, v) = \begin{cases} \prod_s (1 - P_D)^{1-u(y_s)} (P_D \tau(s, y_s))^{u(y_s)} & v = 1 \\ \prod_s V^{-u(y_s)} & v = 0 \end{cases}, \tag{7}$$

$$u(y_s) = \begin{cases} 1 & y_s > 0 \\ 0 & y_s = 0 \end{cases}, \tag{8}$$

where V and τ denote the volume of the surveillance area and the filter-based likelihood function. τ is defined as

$$\tau(s, y_s) = N(y_s; h(x_{s|s-1}), S), \tag{9}$$

where h[1] and S represent the measurement function and innovation uncertainty. Finally, the tuple, $a = \{y_k, ..., y_{k-S+2}\}$, minimizing the cost function is used to update prior estimates $X^n_{k|k-1}, ..., X^n_{k-S+2|k-S+1}$.

7 Road Network Constrained Filtering

In a given scenario, we aim to cover all possible paths a target can follow in a particular time step so that we can collect target spectral data in prediction-based sampling. On a straight road there is no need for assigning a turn model since the likelihood of a manuever is extremely low and noise can account of non-straight paths. On the other hand, on an intersection a target is very likely to change its direction. For this reason, in this paper, specific motion models are adaptively removed/inserted in the GSF based on the external intersection map. OpenStreetMap data-based intersection extraction is given extensive treatment in [3].On a straight road, the Stop model is employed in about 10% of the Gaussians whereas the remaning ones are given the Constant Velocity (CV) model with low or high amount of noise to account for rapid or slow accelarations [6]. Meanwhile, in the intersections, around 60% of the Gaussians are applied left or right turn models whereas the other 30% and 10% are applied the CV and Stop models [9].

8 Simulation Results

We focus on three metrics to evalute tracking and identification performance in the given scenarios. First, the Root Mean Square Error (RMSE) metric is considered to measure positioning accuracy in East-North-Up (ENU) real world coordinates since we utilize this coordinate system in DIRSIG simulation.

[1] In this study we use a linear measurement model since the measurements are extracted in cartesian coordinates. The measurement model considers the central coordinates and physical dimensions of a blob.

The second performance metric is track purity (TP). It measures how many frames a tracker maintains a correct track identity within an estimated gate of the actual target position during the track life. Finally, the Current Assignment Ratio (CAR) metric is utilized to measure the ratio of maximum number of times a ground truth is associated to a track to the duration of ground truth. Details on these metrics can be found in [2].

The proposed spectral feature-aided tracking (SFAT) system is compared to a (1) kinematic only tracker (KT) and a (2) spectral only tracker (ST). This way, the benefit of further reduction of validated measurements in target identification is evaluated. In the KT method, spectral features are ignored whereas in the ST, only SAM scores in the last scan, k, are considered. In the SFAT and KT cases, experiments are performed with $S = 6$ in the S-D assignment algorithm as it is a widely accepted value in the literature. The number of Gaussians in the GSF is 33 in all cases. Obviously, more Gaussians can be employed to better approximate true target density at a higher computational cost. A hundred Monte Carlo runs were carried out for each TOI. A track is terminated when it has not been associated with any measurement for more than 7 s. Fig. 6 displays the RMSE results whereas table 1 displays TP and CAR scores.

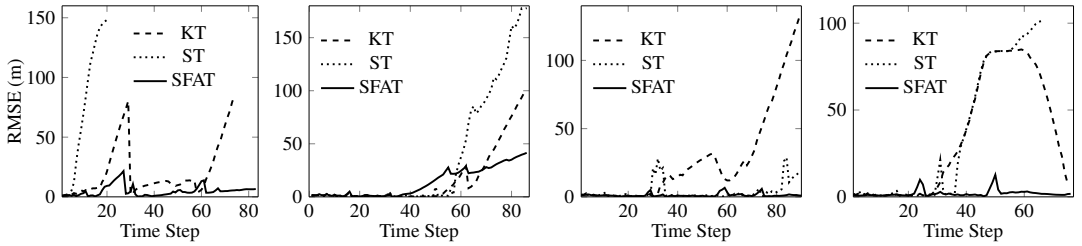

Figure 6: RMSE results for the 1*st* (a), 2*nd* (b), 3*th* (c), and 4*th* (d) TOI.

	Track Purity (%)					Current Assignment Ratio (%)				
Tracker/ID	1st	2nd	3th	4th	Overall	1st	2nd	3th	4th	Overall
KT (6-D)	49.03	77.82	38.05	38.37	50.82	20.85	70.52	36.70	37.45	41.38
ST (2-D)	20.01	65.04	87.48	50.24	55.69	4.82	65.04	87.48	43.63	50.24
SFAT (6-D)	80.14	81.89	94.61	89.63	86.57	70.80	81.09	94.26	89.63	83.95

Table 1: TP and CAR scores for TOIs. Reasonable SAM threshold values were used in the experiments. (1*st* TOI Threshold - 0.05, 2*nd* TOI Threshold - 0.15, 3*th* TOI Threshold - 0.15, 4*th* TOI Threshold - 0.25)

The KT method suffers from vehicles with similar trajectories in cluttered scenes. In addition, severe obscurations have a higher impact on the KT than the SFAT and ST. On the other hand, the SFAT and ST handle these challenges by eliminating vehicles with similar trajectories utilizing the spectral signatures. Furthermore, if we can capture spectral features from the obscured target once it becomes visible, then we can re-associate the track with the true measurements. The ST method performs poorly in scenarios with many vehicles having similar paint models regardless of their kinematic features. The SFAT method accomplishes higher tracking rates since it utilizes kinematic features in a scene with many similar vehicles. It performs relatively poor in the first TOI case due to the very high density of

spectrally similar vehicles to the TOI.

One major drawback of the current feature-aided method is its sensitivity to the spectral threshold. A proper threshold for the first (white) car does not work well for the other TOIs (red, blue, red). As seen in table 2, tracking rates for the first TOI drop dramatically for the threshold values 0.15, 0.2, 0.25, and 0.3. On the other hand, for the other TOIs, 0.15 is the global optimum value in terms of overall rates. Main reason for this sensitivity is that the radiometric sampling process is a function of the sensor reaching radiance magnitude. Therefore, spectral data is effected by a lesser amount of noise for the first TOI than the others due to its higher signal level. This leads to sensitivity in the spectral threshold. By comparing the table 2 to table 1, one can notice that $4-D$ assignment algorithm outperforms the $6-D$ one in the first TOI case. The main reason behind this is the severe occlusions in the scene. If the sufficient prior estimates at time $k-S+1$ are not corrected, then the filter diverges. In this case, the algorithm is more vulnerable and likely to assign a false tuple. Therefore, there is no guarantee of more persistent tracking with the increasing number of dimensions in the $S-D$ assignment algorithm.

Spectral Feature-Aided Tracking										
	Track Purity (%)					Current Assignment Ratio (%)				
Threshold	1st	2nd	3th	4th	Overall	1st	2nd	3th	4th	Overall
0.05	88.43	14.29	14.28	100.00	54.25	88.43	1.16	1.11	9.21	24.98
0.10	68.80	87.36	14.51	94.27	66.24	65.59	86.46	1.24	92.39	61.42
0.15	51.71	77.04	97.11	95.07	80.23	40.39	76.05	97.11	95.07	77.16
0.20	46.89	80.09	73.48	92.17	73.16	25.25	80.09	65.42	91.24	65.50
0.25	8.28	79.80	76.88	88.36	63.33	7.27	79.34	69.60	88.36	61.14
0.30	6.96	79.63	15.44	72.52	43.64	6.36	77.93	14.36	69.71	42.09

Table 2: TP and CAR scores for the SFAT with different SAM thresholds. (4-D assignments)

9 Conclusions

Inserting spectral features in a wide area air-to-ground surveillance system can increase the persistency of tracking in cases where a single modality struggles. For this reason, we consider an adaptive multi-modal performance-driven sensor capable of adaptive spectral data acquisition. Discriminative spectral features are inserted into the tracking algorithm to exclude outliers in data association. This way, cost minimization problem is simplified and false assignments are reduced. In addition, only around 1.5% of the spectral data of the full scene is collected in each revisit, which makes real time spectral data-based tracking feasible as long as it does not require high frame rate. One current issue, however, is the feature-aided system is highly sensitive to the emprical spectral threshold. In the future, we plan on fusing spectral and kinematic likelihoods in a Bayesian fashion to decrease the sensitivy of the spectral threshold in feature matching without degrading tracking accuracy rates.

10 Acknowledgements

This work is supported by the Dynamic Data Driven Applications Systems Program, Air Force Office of Scientific Research, under Grant FA9550-11-1-0348.

References

[1] M Sanjeev Arulampalam, Neil Gordon, Matthew Orton, and Branko Ristic. A variable structure multiple model particle filter for GMTI tracking. In *Information Fusion, 2002. Proceedings of the Fifth International Conference on*, volume 2, pages 927–934. IEEE, 2002.

[2] Erik P Blasch and Pierre Valin. Track purity and current assignment ratio for target tracking and identification evaluation. In *Information Fusion (FUSION), 2011 Proceedings of the 14th International Conference on*, pages 1–8. IEEE, 2011.

[3] Bin Chen, Weihua Sun, and Anthony Vodacek. Improving image-based characterization of road junctions, widths, and connectivity by leveraging OpenStreetMap vector map. In *Geoscience and Remote Sensing Symposium (IGARSS), 2014 IEEE International*, pages 4958–4961. IEEE, 2014.

[4] Somnath Deb, Murali Yeddanapudi, Krishna Pattipati, and Yaakov Bar-Shalom. A generalized SD assignment algorithm for multisensor-multitarget state estimation. *Aerospace and Electronic Systems, IEEE Transactions on*, 33(2):523–538, 1997.

[5] Emmett J Ientilucci and Scott D Brown. Advances in wide-area hyperspectral image simulation. In *AeroSense 2003*, pages 110–121. International Society for Optics and Photonics, 2003.

[6] T Kirubarajan and Y Bar-Shalom. Tracking evasive move-stop-move targets with a GMTI radar using a VS-IMM estimator. *Aerospace and Electronic Systems, IEEE Transactions on*, 39(3):1098–1103, 2003.

[7] Thiagalingam Kirubarajan, Yaakov Bar-Shalom, Krishna R Pattipati, and Ivan Kadar. Ground target tracking with variable structure IMM estimator. *Aerospace and Electronic Systems, IEEE Transactions on*, 36(1):26–46, 2000.

[8] Daniel Krajzewicz, Georg Hertkorn, C Rössel, and P Wagner. Sumo (simulation of urban mobility). In *Proc. of the 4th middle east symposium on simulation and modelling*, pages 183–187, 2002.

[9] X Rong Li and Vesselin P Jilkov. Survey of maneuvering target tracking. Part I. Dynamic models. *Aerospace and Electronic Systems, IEEE Transactions on*, 39(4):1333–1364, 2003.

[10] Reed D Meyer, Kevin J Kearney, Zoran Ninkov, Christopher T Cotton, Peter Hammond, and Bryan D Statt. RITMOS: a micromirror-based multi-object spectrometer. In *Astronomical Telescopes and Instrumentation*, pages 200–219. International Society for Optics and Photonics, 2004.

[11] Oliver Payne and Alan Marrs. An unscented particle filter for GMTI tracking. In *Aerospace Conference, 2004. Proceedings. 2004 IEEE*, volume 3. IEEE, 2004.

[12] Aubrey B Poore. Multidimensional assignment formulation of data association problems arising from multitarget and multisensor tracking. *Computational Optimization and Applications*, 3(1):27–57, 1994.

[13] Andrew Rice, Juan Vasquez, Michael Mendenhall, and John Kerekes. Feature-aided tracking via synthetic hyperspectral imagery. In *Hyperspectral Image and Signal Processing: Evolution in Remote Sensing, 2009. WHISPERS'09. First Workshop on*, pages 1–4. IEEE, 2009.

[14] Jeongho Shin, Sangjin Kim, Sangkyu Kang, Seong-Won Lee, Joonki Paik, Besma Abidi, and Mongi Abidi. Optical flow-based real-time object tracking using non-prior training active feature model. *Real-Time Imaging*, 11(3):204–218, 2005.

[15] Abhijit Sinha, Thiagalingam Kirubarajan, and Yaakov Bar-Shalom. Autonomous ground target tracking by multiple cooperative UAVs. In *Aerospace Conference, 2005 IEEE*, pages 1–9. IEEE, 2005.

[16] Burak Uzkent, M Hoffman, Anthony Vodacek, and Bin Chen. Feature Matching with an Adaptive Optical Sensor in a Ground Target Tracking System. *IEEE Sensors Journal*, 15(1):510–519, 2015.

[17] Burak Uzkent, Matthew J Hoffman, Anthony Vodacek, John P Kerekes, and Bin Chen. Feature Matching and Adaptive Prediction Models in an Object Tracking DDDAS. *Procedia Computer Science*, 18:1939–1948, 2013.

[18] Junqiu Wang and Yasushi Yagi. Integrating color and shape-texture features for adaptive real-time object tracking. *IEEE Transactions on Image Processing*, 17(2):235–240, 2008.

[19] Huiyu Zhou, Yuan Yuan, and Chunmei Shi. Object tracking using SIFT features and mean shift. *Computer vision and image understanding*, 113(3):345–352, 2009.